Single-Component Organic Conductors Based on Neutral Radicals Containing the Pyrazino-TCNQ Skeleton

Yoshiaki Tsubata, Takanori Suzuki, and Tsutomu Miyashi*

Department of Chemistry, Faculty of Science, Tohoku University, Sendai 980, Japan

Yoshiro Yamashita

Institute for Molecular Science, Okazaki 444, Japan

Received April 28, 1992

Pyrazino-TCNQ (**1a**) prepared from 5,8-diiodoquinoxaline (**4a**) is, like TCNQ itself, a strong electron acceptor and gives a stable anion radical salt as well as highly conductive charge-transfer crystals with donors. Substituted derivatives **1b–i** were similarly prepared from 3,6-diiodo-1,2-phenylenediamine (**5**) as a common intermediate, and bulky substituents such as the phenyl or pyridyl groups have very little effect on either the redox properties or planar geometry of **1a**. Neutral radicals **3d–g** derived from pyridyl-substituted derivatives **1d–g**, respectively, are open-shell donor-π-acceptor systems with high electrical amphotericity designed as a new motif for single-component organic conductors. The powder conductivity of **3f** was as high as 3.2 × 10^{-5} S cm^{-1}.

Since the discovery of metallic behavior in charge-transfer (CT) crystals of tetrathiafulvalene (TTF) and tetracyanoquinodimethane (TCNQ),[1] the chemistry of molecular conducting materials has been widely developed.[2] The first organic superconductor consisted of the cation radical salts of tetramethyltetraselenafulvalene (TMTSF)[3] containing a closed-shell counteranion in a 2:1 molar ratio. To date more than 30 examples of ion radical salts and CT crystals have been shown to exhibit superconducting behavior at low temperatures.[4] All of the above-mentioned materials consist of more than two species which are responsible for the conduction of electrons in the solid. On the other hand, considerable attention has also been focused on single-component conducting materials. Because organic solids are usually good insulators, the search for such compounds is a particularly challenging problem in the field of materials chemistry. Recently several papers have reported the semiconducting behavior of single-component organic solids. Noteworthy examples include a series of tetrakis(alkylthio)-TTF[5] and its heavier chalcogen derivatives using the "fastener effect" of long alkyl chains, *p*-quinobis(1,3-dithiole)s exhibiting strong intermolecular interactions through fused heterocycles,[6] and the stable heterocyclic diradicals such as 1,4-phenylenebis(diselenadiazolyl).[7]

One of the difficulties encountered in studies of these new materials is the question of whether the observed conductivity is intrinsic or extrinsic.[7,8] In order to obtain intrinsic conductivity, open-shell molecules containing both

Scheme I

3d
(Form A)

3d
(Form B)

3d
(Form C)
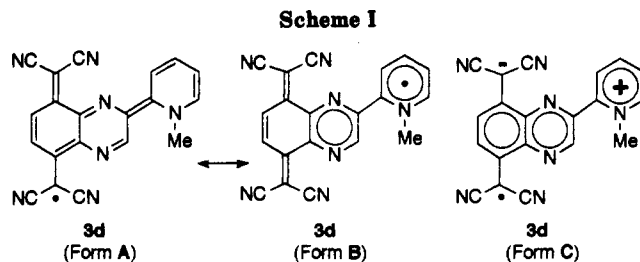
donor and acceptor moieties[9] would seem attractive because these species are electrically amphoteric and conduction electrons can be supplied by charge transfer. With these considerations in mind, neutral radicals such as **3d** were designed as a new motif for single-component organic conductors. As depicted in Scheme I, forms A and B are canonical structures for radical **3d**, and the unpaired electron can be delocalized over the large π-electron system. Form C is a zwitterionic contributor to **3d**, which is formed by electron transfer from the *N*-methylpyridyl radical to the TCNQ skeleton in form B. It is noteworthy that forms B and C are open-shell donor-π-acceptor systems and that fractional charge transfer on the TCNQ skeleton is achieved by contributions from both of them. The pyrazine ring fused to the TCNQ skeleton may be useful as a spacer which is essential to the construction of planar π-electron systems. Removal of the pyrazine spacer in **3d** causes rotation of the pyridyl group as well as butterfly-shaped deformation of the TCNQ moiety due to severe steric repulsions between the cyano group and the pyridyl moiety. Thus, the pyrazino-TCNQ skeleton appears to be a useful π-system which allows the introduction of various functional groups without disturbing the inherent redox properties and planar geometry of TCNQ. In the first portion of this report the redox properties and molecular geometry of pyrazino-TCNQs (**1**) are presented in comparison with those of TCNQ. The neutral radicals **3d–g** are characterized in the second portion, and the validity of our molecular design strategy is discussed.

(1) Ferraris, J.; Cowan, D. O.; Walatka, V., Jr.; Perlstein, J. H. *J. Am. Chem. Soc.* **1973**, *95*, 948.

(2) Bechgaard, K. In *Structure and Properties of Molecular Crystals*; Organic Conductors; Pierrot, M., Ed.; Elsevier: Amsterdam, 1990; pp 235–295.

(3) Bechgaard, K.; Jacobsen, C. S.; Mortensen, K.; Pedersen, H. J.; Thorup, N. *Solid State Commun.* **1980**, *33*, 1119. Jérome, D.; Mazaud, A.; Ribault, M.; Bechgaard, K. *J. Phys. Lett.* **1980**, *41*, L95.

(4) For a recent review: Inokuchi, H. *Angew. Chem., Int. Ed. Engl.* **1988**, *27*, 1747.

(5) Inokuchi, H.; Saito, G.; Wu, P.; Seki, K.; Tang, T. B.; Mori, T.; Imaeda, K.; Enoki, T.; Higuchi, Y.; Inaka, K.; Yasuoka, N. *Chem. Lett.* **1986**, 1263. The high mobility conducting behavior in tetrakis(methyltellura)-TTF was accounted for by partial covalent bonding through the close Te–Te contacts in the crystal. Inokuchi, H.; Imaeda, K.; Enoki, T.; Mori, T.; Maruyama, Y.; Saito, G.; Okada, N.; Yamochi, H.; Seki, K.; Higuchi, Y.; Yasuoka, N. *Nature* **1987**, *329*, 6134.
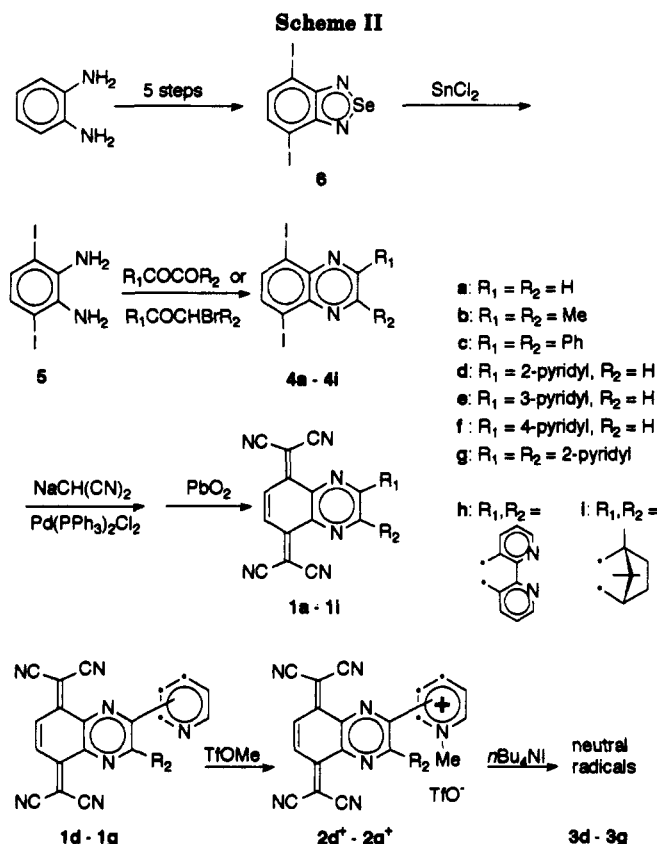
(6) Yamashita, Y.; Tanaka, S.; Imaeda, K.; Inokuchi, H. *Chem. Lett.* **1991**, 1213.

(7) Cordes, A. W.; Haddon, R. C.; Oakley, R. T.; Schneemeyer, L. F.; Waszczak, J. V.; Young, K. M.; Zimmerman, N. M. *J. Am. Chem. Soc.* **1991**, *113*, 582.

(8) West, R.; Jorgenson, J. A.; Stearley, K. L.; Calabrese, J. C. *J. Chem. Soc., Chem. Commun.* **1991**, 1234.

(9) Closed-shell donor–σ-acceptor systems have been prepared for the controlling of stoichiometry in CT crystals or for the investigation of new conducting materials and unimolecular devices. Becker, J. Y.; Bernstein, J.; Bittner, N.; Levi, N.; Shaik, S. S. *J. Am. Chem. Soc.* **1983**, *105*, 4468. Heywang, G.; Born, L.; Fitzky, H.; Hassel, T.; Hocker, J.; Müller, H.; Pittel, B.; Roth, S. *Angew. Chem., Int. Ed. Engl.* **1989**, *28*, 483. Buchwalter, S. L.; Iyenger, R.; Viehbeck, A.; O'Toole, T. R. *J. Am. Chem. Soc.* **1991**, *113*, 376. Metzger, R. M.; Panetta, C. A. *New J. Chem.* **1991**, *15*, 209.
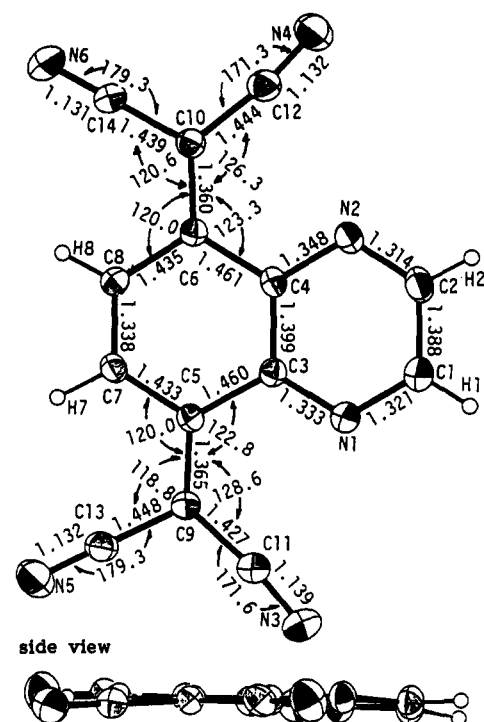
Scheme II

Figure 1. Thermal ellipsoid of pyrazino-TCNQ (1a) on the best molecular plane with selected bond lengths and angles. The side view results from a 90° rotation around the horizontal axis. Other important angles are as follows: N(1)–C(3)–C(4), 121.6°; N-(1)–C(3)–C(5), 118.2°; C(4)–C(3)–C(5), 120.0°; N(2)–C(4)–C(3), 121.0°; N(2)–C(4)–C(6), 118.0°; C(3)–C(4)–C(6), 120.8°; C(3)–C-(5)–C(7), 117.1°; C(4)–C(6)–C(8), 116.5°; C(11)–C(9)–C(13), 112.4°; C(12)–C(10)–C(14), 113.0°.

Table I. Reduction Potentials[a] and Semiquinone Formation Constants (K_{sem})[b] of Pyrazino-TCNQs 1a–i

	E_1^{red}	E_2^{red}	log K_{sem}[b]
1a	+0.23	−0.32	9.48
1b	+0.18	−0.39	9.83
1c	+0.25	−0.29	9.31
1d	+0.25	−0.30	9.48
1e	+0.24	−0.30	9.31
1f	+0.26	−0.28	9.31
1g	+0.25	−0.29	9.31
1h	+0.25	−0.28	9.13
1i	+0.18	−0.39	9.83
TCNQ	+0.28	−0.29	9.83

[a] Measured by cyclic voltammetry in dry DMF, E/V vs SCE, 0.1 mol dm^{-3} Et$_4$NClO$_4$ as a supporting electrolyte, Pt wire electrode. The oxidation potential of ferrocene is +0.44 V under the same conditions. [b] K_{sem} = $[1^-]^2/[1^0][1^{2-}]$, log K_{sem} = (E_1^{red} − E_2^{red})/0.058.
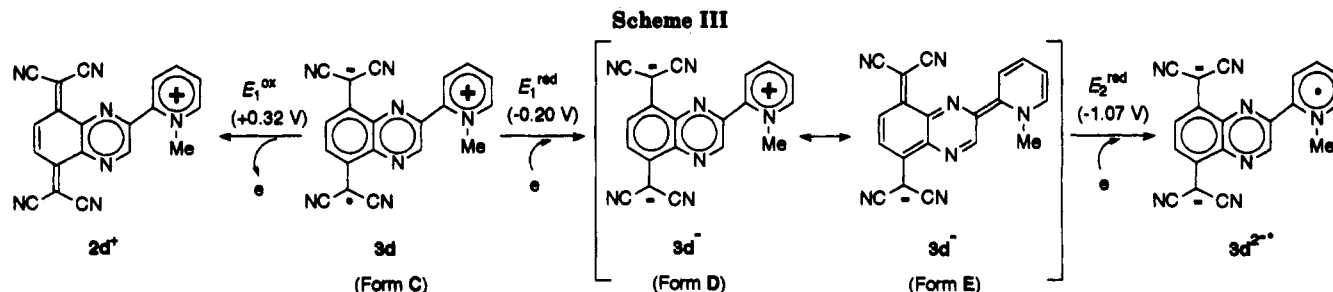
Results and Discussion

Preparation and Molecular Structure of Pyrazino-TCNQs. 3,6-Diiodo-1,2-phenylenediamine (5) was chosen as a key synthon and prepared by the reductive ring opening of 4,7-diiodobenzo[c][1,2,5]selenadiazole (6) in 93% yield. Because the direct iodination of benzo[c]-[1,2,5]selenadiazole gave 6 in low yield,[10] another preparation was pursued, and 6 was finally obtained in 53% yield from 1,2-phenylenediamine in five steps. As shown in Scheme II, condensation of diamine 5 with glyoxal gave 5,8-diiodoquinoxaline (4a) in 57% yield which was subjected to Takahashi's phenylenebismalononitrile preparation.[11] Subsequent oxidation of the dihydro derivative gave pyrazino-TCNQ (1a) in 29% yield. Various substituents were introduced on the pyrazine ring by the condensation reactions of diamine 5 with the corresponding α,β-diketones or α-bromo ketones, giving substituted diiodoquinoxalines 4b–i in 20–91% yields. From these, substituted pyrazino-TCNQs 1b–i were similarly prepared in 12–81% yields.

The X-ray structure determination revealed that, in the solid state at least, the annelation of a pyrazine ring has little effect on the molecular planarity of TCNQ.[12] This result stands in contrast to the annelation of a benzene ring, which causes a butterfly-shaped deformation of the TCNQ skeleton due to severe steric repulsions between the cyano groups and the hydrogens at the peri positions.[13] As shown in Figure 1, 1a possesses a planar geometry with the largest deviation (0.29 Å out of the molecular plane) occurring at the cyano nitrogen N6. Slight deformation of the TCNQ skeleton was observed as the bowing of two

cyano groups in the molecular plane [N3–C11–C9, 171.6 (3)° and N4–C12–C10, 171.3 (3)°] as well as the widening of the bond angles of C5–C9–C11 [128.6 (3)°] and C6–C10–C12 [126.3 (3)°], which may be due to the steric interaction between the cyano groups and the pyrazine lone pairs.[14]

Redox Properties of Pyrazino-TCNQs. Cyclic voltammograms of 1a–i showed two pairs of reversible waves. The first and second reduction potentials (E_1^{red}, E_2^{red}), summarized in Table I, indicate that they are strong electron acceptors as is TCNQ. It is noteworthy that 1a–i possess nearly the same reduction potentials, showing that

(10) Bird, C. W.; Cheeseman, G. W. H.; Sarsfield, A. A. *J. Chem. Soc.* **1963**, 4767.

(11) Uno, M.; Seto, K.; Masuda, M.; Ueda, W.; Takahashi, S. *Tetrahedron Lett.* **1985**, *26*, 1553.

(12) Long, R. E.; Sparks, R. A.; Trueblood, K. N. *Acta Crystallogr.* **1965**, *18*, 932.

(13) Iwasaki, F. *Acta Crystallogr. Sect. B* **1971**, *27*, 1360.

(14) Recently, an attractive interaction between a cyano group and a pyridine lone pair was reported in 2,2'-bipyridine-3,3'-dicarbonitrile. The very similar atomic arrangement in 1a suggests that such an interaction is also at work in 1a. Baxter, P. N. W.; Connor, J. A.; Povey, D. C.; Wallis, J. D. *J. Chem. Soc., Chem. Commun.* **1991**, 1135.

Scheme III

a bulky substituent such as the phenyl or pyridyl group does not affect the redox properties of the pyrazino-TCNQ skeleton. Lower values of 1b and 1i are the result of electron-donating properties of alkyl substituents.

Reductions of 1a–c with iodide ion afforded blue-green anion radical species which could be isolated as stable salts. These anion radicals exhibit strong absorption maxima in the visible region [1a$^-$: λmax (MeCN) = 834 (log ϵ 4.23), 642 (4.67), 595 (4.21) nm] much like TCNQ$^-$.[15] Highly conductive CT crystals were obtained by the direct combination of 1a with TTF or TMTSF in CH$_2$Cl$_2$, and their powder conductivities were 1.4 and 0.91 S cm^{-1}, respectively.[16] Because of the high conductivities and the 1:1 donor-to-acceptor ratio, partial charge transfer must occur in these solids. CT crystals of 1a with other donors or those of 1b and 1c were similarly obtained by the direct method, although their conductivities were low.

All of the results obtained clearly show that pyrazino-TCNQ (1a) maintains the intriguing properties of TCNQ. Furthermore, functionalization of the acceptor skeleton can be achieved more easily in pyrazino-TCNQ than in TCNQ, because the inherent redox properties of the skeleton are perturbed by introducing a large substituent in the latter but remain essentially unchanged in the former. The geometry of the TCNQ skeleton suffers from the steric interactions of substituents as exemplified by the severely deformed structure of tetramethyl-TCNQ.[17] On the other hand, bulky substituents have very little effect on the pyrazino-TCNQ skeleton, and various functional groups such as a chiral auxiliary in 1i ([α]$_D$ +24°) could be introduced by using 5 as a common intermediate, allowing the systematic investigation of functionalized acceptors.

Preparation and Properties of Neutral Radicals. Quaternizations of the pyridyl substituent in 1d–g with methyl triflate afforded N-methylated cations 2d$^+$–g$^+$, respectively (Scheme II), which underwent three-stage one-electron reductions (Table II). Slightly higher values of E_1^{red} and E_2^{red} for these cations compared to those of 1d–g are due to the strong electron-withdrawing power of the N-methylpyridinium group.[18] The third reduction potentials (E_3^{red}) are close to E_1^{red} of N-methylpyridinium (-1.27 V). These results suggest that E_1^{red} and E_2^{red} of 2d$^+$–g$^+$ correspond to the reduction of the pyrazino-TCNQ skeleton whereas the N-methylpyridinium moiety is reduced at E_3^{red}. Thus, the main contributor to the neutral radicals 3d–g may be considered to be the zwitterionic

Table II. Redox Potentials[a] of Cations 2d$^+$–g$^+$ and Radicals 3d–g

	E_1^{ox}	E_1^{red}	E_2^{red}	E_3^{red}
2d$^+$		+0.32	-0.20	-1.07^b
3d	+0.32	-0.20	-1.05^b	
2e$^+$		+0.31	-0.21	-1.22^b
3e	+0.32	-0.20	-1.21^b	
2f$^+$		+0.31	-0.22	-1.02
3f	+0.33	-0.22	-1.00	
2g$^+$		+0.35	-0.19	-1.27^b
3g	+0.36	-0.18	-1.26^b	

[a] Measured by cyclic voltammetry in dry DMF, E/V vs SCE, 0.1 mol dm^{-3} Et$_4$NClO$_4$ as a supporting electrolyte, Pt wire electrode. Triflate salts were used for the measurements of 2d$^+$–g$^+$. N-Methylpyridinium iodide underwent irreversible reduction at -1.27 V under the same conditions. [b] Irreversible waves.
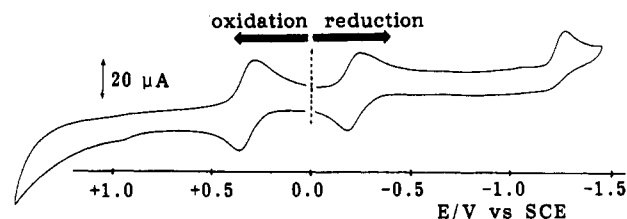
Figure 2. Cyclic voltammogram of radical 3e in DMF.

structure, form C, in which the unpaired electron is localized on the pyrazino-TCNQ skeleton.

Reactions of the triflate salts of 2d$^+$–g$^+$ with n-Bu$_4$NI in MeCN gave neutral radicals 3d–g as stable black-violet powders with very low solubilities. Cyclic voltammograms of 3d–g indicated that they underwent facile and reversible one-electron oxidation as well as two-stage one-electron reductions, demonstrating their electrochemical amphotericity (Figure 2). As shown in Table II, the oxidation potentials (E_1^{ox}) of 3d–g correspond well to E_1^{red} of 2d$^+$–g$^+$ as expected, and E_1^{red} and E_2^{red} of 3d–g are the same as E_2^{red} and E_3^{red} of 2d$^+$–g$^+$, respectively. From the redox properties of 3d–g it was confirmed that these species exist as monomers rather than as covalently bound dimers.[19]

It is noteworthy that the values for E_2^{red} of 3d and 3f are higher by ca. 0.2 V than those of 3e and 3g or than E_1^{red} of N-methylpyridinium. As shown in Scheme III, this difference suggests that there is effective conjugation between the 2- or 4-pyridyl moiety and the pyrazino-TCNQ skeleton in form D and can be accounted for by considering form E as an additional contributor in 3d$^-$ and 3f$^-$. A contribution from form E cannot be expected in the 3-pyridyl derivative 3e$^-$, however, and may be precluded in 3g$^-$ by rotation of the 2-pyridyl moieties due to steric interactions between the vicinal substituents.

The contribution of form C in the radicals was evidenced by the considerable resemblance between the visible spectra of 3 and 1a$^-$, suggesting that the SOMO of 3 is similar to that of 1a$^-$. On the other hand, the LUMO of

(15) Absorption maxima of TCNQ$^-$ in MeCN are 842, 760, 744, 680, and 665 nm. Melby, L. R.; Harder, R. J.; Hertler, W. R.; Mahler, W.; Benson, R. E.; Mochel, W. E. *J. Am. Chem. Soc.* **1962**, *84*, 3374.

(16) Conductivities were measured on compaction pellets by a two-probe method at room temperature. That of TTF·TCNQ is 2.7 S cm^{-1} under the same conditions.

(17) Rosenau, B.; Krieger, C.; Staab, H. A. *Tetrahedron Lett.* **1985**, *26*, 2081. Kini, A.; Mays, M.; Cowan, D. *J. Chem. Soc., Chem. Commun.* **1985**, 286.

(18) Relatively small substituent effects on E_1^{red} and E_2^{red} of pyrazino-TCNQ may be due to the small LCAO coefficients at C$_2$ and C$_3$ in LUMO of 1a.

(19) Dong, V.; Endres, H.; Keller, H. J.; Moroni, W.; Nöthe, D. *Acta Crystallogr. Sect. B* **1977**, *33*, 2428.
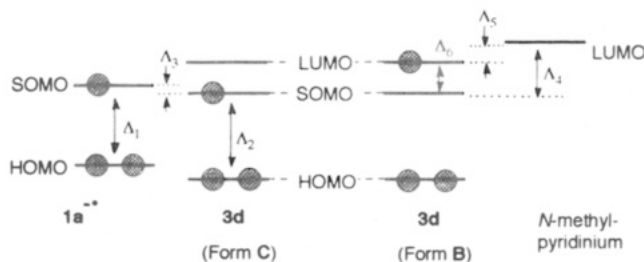
Figure 3. Qualitative scheme of energy diagram. Energy differences are estimated as follows: Δ_1, 2.58 eV, from the end absorption (480 nm) of **1a**; Δ_2, 2.64 eV, from the end absorption (470 nm) of **2d**$^+$; Δ_3, 0.09 eV, from the difference of E_1^{ox} of **1a**$^{·-}$ and **3d** (i.e., E_1^{red} of **1a** and **2d**$^+$); Δ_4, 1.59 eV, from the difference of E_1^{red} of **2d**$^+$ and *N*-methylpyridinium; Δ_5, > 0.2 eV ?, from the difference of E_2^{red} **3d** and E_1^{red} of *N*-methylpyridinium; Δ_6, 0.95 eV ?, from the very weak NIR absorption of **3d** in 1200–1400-nm region.

3 may possess large coefficients in the *N*-methylpyridinium moiety, so that a contribution by form **B** is expected by configuration interaction (CI). The qualitative diagram shown in Figure 3 was obtained by comparisons of UV–vis spectra and redox potentials. The contribution of form **A**, a canonical structure of form **B**, is expected only in **3d** and **3f**, which may increase the contribution from CI in **3d** and **3f** but not in **3e** and **3g**. Thus, the achievement of fractional charge transfer on the pyrazino-TCNQ skeleton appears to be easier in **3d** and **3f** than in **3e** and **3g**. Such differences in electronic structure may be more favored for the higher conductivities in **3d** and **3f** than in **3e** and **3g**.

The powder conductivities of **3d**–**g** are much higher than is usual for organic solids, with values of 8.5×10^{-9}, 9.1×10^{-6}, 3.2×10^{-5}, and 2.3×10^{-7} S cm^{-1}, respectively. The value for **3f** is comparable to those reported for other single-component semiconductors.[5–7] Although these values are lower than the highly conductive CT crystals of **1a** or other multicomponent organic conductors, radicals studied in this work provide a new example of single-component organic conductors. On the other hand, the effect of substituted positions on the electronic structures in **3d**–**f** does not reflect the order of electrical conductivities. Because electrical conduction is a property of molecular assemblies, this disagreement can be rationalized by assuming different packing arrangements for the molecules in the various crystals.

The present study reveals that open-shell donor-π-acceptor systems constitute a promising approach to the study of single-component organic conductors. The designation of intrinsic conductivity is warranted in this case because of the presence of conduction electrons, available in open-shell species with electrical amphotericity, which form the core of our molecular design. Furthermore, it is possible to prepare a single-component organic solid that shows metallic behavior by decreasing the SOMO–LUMO gap of the radical to zero.

Accordingly, our efforts to extend this work have been directed toward molecules possessing narrow SOMO–LUMO gaps. Annelation of the cationic moiety to the pyrazino-TCNQ skeleton may cause greater mixing of their LUMOs, thus producing the promising cationic precursor for the radical with high conductivity. Quaternization of **1h** gave the *N*-methylphenanthrolinium derivative (**2h**$^+$); however, the very low solubility of **1h** in common solvents prevented the isolation of **2h**$^+$ salts in pure form.[20] An-

other strategy to narrow the gap consists of the exchange of the TCNQ acceptor and/or the pyridinium pendant in the cationic precursor, respectively, for much weaker acceptor skeletons and/or cationic pendants with stronger electron affinities. Studies in this vein are now in progress.

Experimental Section

General. Melting points are reported uncorrected. All the IR spectra were taken in KBr disks. Mass spectra were obtained in EI mode unless otherwise indicated.

Preparation of 3,6-Diiodo-1,2-phenylenediamine (5). 4,7-Dibromobenzo[*c*][1,2,5]thiadiazole (**9**) was prepared from 1,2-phenylenediamine according to the literature[21] and obtained in 78% yield over two steps. To a suspension of **9** (15.3 g, 52.0 mmol) in EtOH (500 mL) was added portionwise sodium borohydride (36.4 g, 0.96 mol) at 0 °C, and the mixture was stirred for 20 h at room temperature. After evaporation of the solvent, 500 mL of water was added, and the mixture was extracted with ether. The extract was washed with brine and dried over anhydrous sodium sulfate. Evaporation of the solvent gave 3,6-dibromo-1,2-phenylenediamine (**8**) (12.0 g) as a pale yellow solid in 87% yield. This preparation of **8** is more convenient than those reported which gave **8** in 5% yield from 1,4-dibromobenzene over two steps[22] or **8**·HCl in 29% yield from benzo[*c*][1,2,5]oxadiazole 1-oxide over three steps.[23]

To a solution of **8** (14.6 g, 54.8 mmol) in refluxing EtOH (300 mL) was added a solution of selenium dioxide (6.30 g, 56.8 mmol) in hot water (120 mL). The mixture was heated under reflux for 2 h. Filtration of the yellow precipitates gave 4,7-dibromobenzo[*c*][1,2,5]selenadiazole (**7**) (16.9 g) in 91% yield. This preparation of **7** is as convenient as the reported method[10] in which benzo[*c*][1,2,5]selenadiazole was allowed to react with bromine by using Ag$_2$SO$_4$ in H$_2$SO$_4$ to give **7** in 62% yield.

A suspension of **7** (10.1 g, 29.8 mmol), KI (87.7 g, 0.53 mol), and CuI (52.2 g, 0.27 mol) in DMSO (500 mL) was heated for 48 h at 130 °C under nitrogen, and the mixture was poured into water (1 L). The resulting brown precipitates were filtered and suspended in 2 L of 28% aqueous NH$_3$. After vigorous stirring for 20 min at room temperature, a yellow powder was filtered, washed with water, and purified by sublimation (220 °C, 1 × 10^{-2} Torr). 4,7-Diiodobenzo[*c*][1,2,5]selenadiazole (**6**) (11.1 g) was obtained as a yellow solid in 86% yield. This preparation of **6** is more convenient than the reported method[10] in which benzo[*c*]-[1,2,5]selenadiazole was allowed to react with iodine by using Ag$_2$SO$_4$ in H$_2$SO$_4$ to give **6** in 10% yield.

A mixture of **6** (1.34 g, 3.09 mmol) and tin(II) chloride dihydrate (4.40 g, 19.5 mmol) was ground in a mortar and was added portionwise to 40 mL of concd HCl. After the mixture was stirred for 3.5 h at room temperature, a black solid was filtered and suspended in 50 mL of 50% aqueous NaOH. After the suspension was stirred for 1 h at room temperature, 100 mL of water was added, and the mixture was extracted with ether. The extract was washed with water and dried over anhydrous sodium sulfate. Evaporation of the solvent followed by recrystallization from chloroform/*n*-hexane gave 3,6-diiodo-1,2-phenylenediamine (**5**) (1.06 g) as pale yellow needles in 93% yield.

5: mp 108–110 °C; IR 3380, 3350, 3300, 3250 cm^{-1}; ^{1}H NMR (90 MHz, CDCl$_3$) δ 6.91 (s, 2 H), 3.91 (br s, 4 H); MS (13.5 eV, 80 °C) *m/z* (relative intensity) 362 (M$^+$ + 2, 12), 361 (M$^+$ + 1, 59), 360 (M$^+$, 100), 233 (M$^+$ – I, 42).

Anal. Calcd for C$_6$H$_6$N$_2$I$_2$: C, 20.02; H, 1.68; N, 7.78; I, 70.52. Found: C, 20.03; H, 1.47; N, 7.80; I, 70.37.

Preparation of 5,8-Diiodoquinoxalines (4) (Method A). To a solution of **5** (300 mg, 0.83 mmol) in 10 mL of EtOH was added 40% aqueous glyoxal (0.12 mL, 1.0 mmol), and the mixture was heated under reflux for 24 h. After evaporation of the solvent, the crude product was washed with MeOH and purified by sublimation (180 °C, 1.0 × 10^{-2} Torr). 5,8-Diiodoquinoxaline (**4a**)

(20) The preliminary study for preparing **3h** from **2h**$^+$MeSO$_4^-$ suggested a powder conductivity of about 10^{-6} S cm^{-1} for **3h**.

(21) Pilgram, K.; Zupan, M.; Skiles, R. *J. Heterocycl. Chem.* **1970**, *7*, 629.

(22) Calhane, D. F.; Wheeler, P. M. *Am. Chem. J.* **1899**, *22*, 449.

(23) Boyer, J. H.; Toggweiler, U.; Stoner, G. A. *J. Am. Chem. Soc.* **1957**, *79*, 1748.

(180 mg) was obtained as a yellow solid in 57% yield.

2,3-Dimethyl- (**4b**), 2,3-diphenyl- (**4c**), and 2,3-di(2-pyridyl)-5,8-diiodoquinoxaline (**4g**), 10,13-diiododipyrido[3,2-*a*:2,3-*c*]phenazine (**4h**), and (1*R*)-(+)-6,9-diiodo-1,11,11-trimethylquinoxalo[*b*]bicyclo[2.2.1]heptene (**4i**) were similarly prepared by the reactions of **5** with diacetyl, benzil, 2,2'-pyridyl, 1,10-phenanthroline-5,6-dione,[24] and (1*R*)-(-)-camphorquinone, respectively, in refluxing EtOH.

4a: mp 234-235.5 °C; IR 1461, 1365, 1160, 1020, 956, 870, 820 cm^{-1}; ^{1}H NMR (90 MHz, CDCl$_3$) δ 8.87 (s, 2 H), 8.04 (s, 2 H); MS (13.5 eV, 100 °C) *m/z* (relative intensity) 383 (M$^+$ + 1, 15), 382 (M$^+$, 100).

Anal. Calcd for C$_8$H$_4$N$_2$I$_2$: C, 25.16; H, 1.06; N, 7.33. Found: C, 25.22; H, 1.11; N, 7.29.

4b: yield 81%, pale yellow needles (chloroform/*n*-hexane); mp 123.5-125.5 °C; IR 1485, 1455, 1360, 1130, 880, 825 cm^{-1}; ^{1}H NMR (90 MHz, CDCl$_3$) δ 8.20 (s, 2 H), 2.81 (s, 6 H); MS (13.5 eV, 90 °C) *m/z* (relative intensity) 411 (M$^+$ + 1, 8), 410 (M$^+$, 100), 282 (M$^+$ - I, 7).

Anal. Calcd for C$_{10}$H$_8$N$_2$I$_2$: C, 29.30; H, 1.97; N, 6.83. Found: C, 29.18; H, 1.87; N, 6.82.

4c: yield 91%, pale yellow leaflets (MeCN); mp 220-220.5 °C; IR 1445, 1410, 1380, 1325, 1020, 980, 890 cm^{-1}; ^{1}H NMR (200 MHz, CDCl$_3$) 8.04 (s, 2 H), 7.50-7.73 (m, 4 H), 7.34-7.42 (m, 6 H); MS (70 eV) *m/z* (relative intensity) 535 (M$^+$ + 1, 25), 534 (M$^+$, 100), 533 (M$^+$ - 1, 24), 407 (M$^+$ - I, 8), 279 (M$^+$ - 2I, 19).

Anal. Calcd for C$_{20}$H$_{12}$N$_2$I$_2$: C, 44.97; H, 2.26; N, 5.24; I, 47.52. Found: C, 44.74; H, 2.26; N, 5.26; I, 47.48.

4g: yield 81%, pale yellow leaflets (1,2-dichloroethane); mp 287-290.5 °C; IR 1000, 788, 740 cm^{-1}; ^{1}H NMR (200 MHz, CDCl$_3$) δ 8.34 (ddd, *J* = 7.8, 1.2, 1.2 Hz, 2 H), 8.29 (ddd, *J* = 4.8, 1.2, 0.8 Hz, 2 H), 8.10 (s, 2 H), 7.93 (ddd, *J* = 7.8, 7.8, 0.8 Hz, 2 H), 7.27 (ddd, *J* = 7.8, 4.8, 1.2 Hz, 2 H); MS (70 eV) *m/z* (relative intensity) 536 (M$^+$, 88), 535 (M$^+$ - 1, 100).

Anal. Calcd for C$_{18}$H$_{10}$N$_4$I$_2$: C, 40.33; H, 1.88; N, 10.45; I, 47.34. Found: C, 40.06; H, 1.89; N, 10.38; I, 47.48.

4h: yield 65%, yellow solid (sublimation, 350 °C, 1 × 10^{-2} Torr); mp >400 °C; IR 1640, 1470, 1410, 1355, 1315, 1120, 980, 805, 740 cm^{-1}; ^{1}H NMR could not be measured because of its low solubility; MS (70 eV) *m/z* (relative intensity) 535 (M$^+$ + 1, 24), 534 (M$^+$, 100), 533 (M$^+$ - 1, 22).

Anal. Calcd for C$_{18}$H$_8$N$_4$I$_2$: C, 40.48; H, 1.51; N, 10.49; I, 47.52. Found: C, 40.41; H, 1.59; N, 10.45; I, 47.27.

4i: yield 77%, pale yellow needles (CH$_2$Cl$_2$/*n*-hexane); mp 181-182 °C; IR 2960, 1370, 1160, 900, 800 cm^{-1}; ^{1}H NMR (200 MHz, CDCl$_3$) δ 7.94 (s, 2 H), 3.25 (d, *J* = 4.2 Hz, 1 H), 2.33 (ddd, *J* = 9.2, 9.2, 4.2 Hz, 1 H), 2.09 (dd, *J* = 9.2, 9.2 Hz, 1 H), 1.34-1.50 (m, 2 H), 1.47 (s, 3 H), 1.14 (s, 3 H), 0.61 (s, 3 H); MS (70 eV) *m/z* (relative intensity) 490 (M$^+$, 100), 475 (17), 447 (29); [α]^{20}$_D$ = +18° (*c* 1.0, CHCl$_3$).

Anal. Calcd for C$_{16}$H$_{16}$N$_2$I$_2$: C, 39.21; H, 3.29; N, 5.72. Found: C, 39.27; H, 3.35; N, 5.76.

Preparation of 5,8-Diiodoquinoxalines (4) (Method B). A solution of **5** (5.30 g, 14.7 mmol) and 2-(bromoacetyl)pyridinium bromide[25] (4.30 g, 15.3 mmol) in dry DMSO (70 mL) was heated for 1 h at 60 °C. The mixture was poured into water and extracted with ether. The extract was washed with brine and dried over anhydrous sodium sulfate. Evaporation of the solvent gave a black-brown solid which was chromatographed on silica gel (1:1 CH$_2$Cl$_2$/*n*-hexane) and further separated by column chromatography on alumina (CH$_2$Cl$_2$). Recrystallization from 1,2-dichloroethane followed by sublimation (190 °C, 1 × 10^{-2} Torr) gave 2-(2-pyridyl)-5,8-diiodoquinoxaline (**4d**) (1.35 g) as a yellow solid in 20% yield. The main byproduct of this reaction was 2-(2-pyridyl)-4,7-diiodobenzimidazole (**10**) obtained in 22% yield.

2-(3-Pyridyl)- (**4e**) and 2-(4-pyridyl)-5,8-diiodoquinoxaline (**4f**) were similarly prepared by the reactions of **5** with 3- and 4-(bromoacetyl)pyridinium bromide,[25] respectively. Chromatographic separation on alumina (9:1 CH$_2$Cl$_2$/ether) was sufficient for the isolation of **4e** and **4f**.

4d: mp 190-195 °C dec; IR 1460, 1160, 1060, 965, 820, 780 cm^{-1}; ^{1}H NMR (200 MHz, CDCl$_3$) δ 9.99 (s, 1 H), 8.80 (dd, *J* = 4.8, 0.8

Hz, 1 H), 8.77 (dd, *J* = 6.0, 1.8 Hz, 1 H), 8.09 (s, 2 H), 7.94 (ddd, *J* = 7.6, 4.8, 1.8 Hz, 1 H), 7.48 (ddd, *J* = 7.6, 6.0, 0.8 Hz, 1 H); MS (25 eV, 80 °C) *m/z* (relative intensity) 460 (M$^+$ + 1, 10), 459 (M$^+$, 100).

Anal. Calcd for C$_{13}$H$_7$N$_3$I$_2$: C, 34.02; H, 1.54; N, 9.15; I, 55.29. Found: C, 34.04; H, 1.64; N, 9.34; I, 55.29.

4e: yield 43%, pale yellow powder (1,2-dichloroethane); mp 240-242 °C dec; IR 1450, 1440, 1305, 1165, 1020, 965, 820, 700 cm^{-1}; ^{1}H NMR (200 MHz, CDCl$_3$) δ 9.56 (br d, *J* = 1.6 Hz, 1 H), 9.38 (s, 1 H), 8.82 (dd, *J* = 5.0, 1.8 Hz, 1 H), 8.71 (ddd, *J* = 8.0, 1.8, 1.6 Hz, 1 H), 8.13 (d, *J* = 7.9 Hz, 1 H), 8.11 (d, *J* = 7.9 Hz, 1 H), 7.57 (dd, *J* = 8.0, 5.0, 1 H); MS (25 eV, 80 °C) *m/z* (relative intensity) 460 (M$^+$ + 1, 59), 459 (M$^+$, 100), 332 (M$^+$ - I, 19), 205 (M$^+$ - 2I, 16).

Anal. Calcd for C$_{13}$H$_7$N$_3$I$_2$: C, 34.02; H, 1.54; N, 9.15. Found: C, 33.$\overline{}$4; H, 1.55; N, 9.16.

4f: yield 47%, pale yellow powder (1,2-dichloroethane); mp 200-201 °C dec; IR 1460, 1300, 1170, 1050, 970, 830 cm^{-1}; ^{1}H NMR (200 MHz, CDCl$_3$) δ 9.37 (s, 1 H), 8.89 (AA'XX', *J*$_{2,3}$ = 6.2 Hz, 2 H), 8.21 (AA'XX', *J*$_{2,3}$ = 6.2 Hz, 2 H), 8.14 (d, *J* = 8.4 Hz, 1 H), 8.13 (d, *J* = 8.4 Hz, 1 H); MS (13.5 eV, 100 °C) *m/z* (relative intensity) 459 (M$^+$, 37), 458 (M$^+$ - 1, 100).

Anal. Calcd for C$_{13}$H$_7$N$_3$I$_2$: C, 34.02; H, 1.54; N, 9.15. Found: C, 33.98; H, 1.82; N, 9.22.

10: colorless crystals, mp 230-231 °C; IR 3400 cm^{-1}; ^{1}H NMR (90 MHz, CDCl$_3$) δ 8.54-8.66 (m, 2 H), 7.80 (ddd, *J* = 7.4, 7.4, 1.8 Hz, 1 H), 7.25-7.50 (m, 3 H); MS (25 eV, 100 °C) (relative intensity) 447 (M$^+$, 15), 446 (M$^+$ - 1, 100), 320 (M$^+$ - I, 69).

Anal. Calcd for C$_{12}$H$_7$N$_3$I$_2$: C, 32.57; H, 1.58; N, 9.40. Found: C, 32.18; H, 1.53; N, 9.71.

Preparation of 5*H*,8*H*-5,8-Bis(dicyanomethylene)-quinoxalines (Pyrazino-TCNQs) (1). Under a nitrogen atmosphere, a suspension of **4a** (824 mg, 2.16 mmol), sodium hydride (60%, oil suspension) (792 mg, 19.8 mmol), Pd(PPh$_3$)$_2$Cl$_2$ (164 mg, 0.233 mmol), and malononitrile (613 mg, 9.28 mmol) in dry THF (30 mL) was heated under reflux for 28 h. The mixture was poured into water (400 mL) and washed with CH$_2$Cl$_2$ (200 mL × 3). The aqueous layer containing the violet dianion of **1a** was acidified with 5% aqueous HCl and extracted with CH$_2$Cl$_2$. The extract was washed with brine. Removal of the solvent gave the dihydro derivative of **1a** as a green solid, which was suspended in benzene (250 mL), EtOH (100 mL), and 5% aqueous HCl (150 mL). The whole mixture was shaken vigorously with PbO$_2$ (10.3 g, 41.8 mmol) for 20 min. The resulting insoluble material was removed through a Celite pad and washed with EtOH and CH$_2$Cl$_2$. The organic layer was separated from the filtrate, and the aqueous layer was extracted with CH$_2$Cl$_2$. The whole organic layer was washed with brine and dried over anhydrous sodium sulfate. Chromatographic separation on silica gel (CH$_2$Cl$_2$) followed by recrystallization from benzene gave 5*H*,8*H*-5,8-bis(dicyanomethylene)quinoxaline (**1a**) (161 mg) as yellow crystals in 29% yield.

2,3-Dimethyl- (**1b**), 2,3-diphenyl- (**1c**), 2-(2-pyridyl)- (**1d**), 2-(3-pyridyl)- (**1e**), 2-(4-pyridyl)- (**1f**), and 2,3-di(2-pyridyl)-pyrazino-TCNQ (**1g**), 10*H*,13*H*-10,13-bis(dicyanomethylene)dipyrido[3,2-*a*:2,3-*c*]phenazine (**1h**), and (1*R*)-(+)-6*H*,9*H*-6,9-bis(dicyanomethylene)-1,11,11-trimethylquinoxalo[*b*]bicyclo[2.2.1]heptene (**1i**) were similarly prepared from the corresponding diiodides **4b**-**i**, respectively. The dihydro derivatives of **1d**-**h** were not isolated because of the low solubility of the dianions in water, and the remaining solids obtained by evaporation of THF were directly oxidized with PbO$_2$.

1a: mp 286-287 °C dec; IR 2214 cm^{-1}; ^{1}H NMR (90 MHz, CDCl$_3$) δ 9.08 (s, 2 H), 7.80 (s, 2 H); UV (MeCN) λmax 390 nm (log ε 4.58), 370 (4.41), 352 (4.11, sh), 313 (3.66), 278 (3.42), 245 (3.54); MS (25 eV, 100 °C) *m/z* 256 (M$^+$).

Anal. Calcd for C$_{14}$H$_4$N$_6$: C, 65.63; H, 1.57; N, 32.80. Found: C, 65.78; H, 1.57; N, 33.07.

1b: yield 22%, yellow crystals (chloroform/*n*-hexane); mp 232-234 °C dec; IR 2219, 2210 cm^{-1}; ^{1}H NMR (90 MHz, CDCl$_3$) δ 7.71 (s, 2 H), 2.81 (s, 6 H); UV (MeCN) λmax 390 nm (log ε 4.62), 372 (4.50, sh), 310 (3.94), 260 (3.83), 251 (3.87, sh), 243 (3.90); MS (25 eV, 100 °C) *m/z* (relative intensity) 285 (M$^+$ + 1, 12), 284 (M$^+$, 100), 283 (M$^+$ - 1, 26), 258 (M$^+$ - CN, 10), 257 (M$^+$ - 1 - CN, 22).

Anal. Calcd for C$_{16}$H$_8$N$_6$: C, 67.60; H, 2.84; N, 29.56. Found: C, 67.54; H, 2.88; N, 29.54.

(24) Dickeson, J. E.; Summers, L. A. *Aust. J. Chem.* **1970**, *23*, 1023.

(25) Wingfield, H. N., Jr. *J. Org. Chem.* **1959**, *24*, 872.

1c: yield 81%, red cubes (1,2-dichloroethane); mp 309–311 °C dec; IR 2213 cm^{-1}; ^{1}H NMR (200 MHz, CDCl$_3$) δ 7.80–7.84 (m, 4 H), 7.77 (s, 2 H), 7.35–7.47 (m, 6 H); UV (MeCN) λmax 392 nm (log ϵ 4.70), 370 (4.63), 354 (4.50, sh), 284 (3.98), 228 (4.36); MS (13.5 eV, 130 °C) m/z (relative intensity) 410 (M$^+$ + 2, 9), 409 (M$^+$ + 1, 72), 408 (M$^+$, 100).

Anal. Calcd for C$_{28}$H$_{12}$N$_6$: C, 76.46; H, 2.96; N, 20.58. Found: C, 76.61; H, 3.13; N, 20.55.

1d: yield 42%, yellow powder (1,2-dichloroethane); mp 258–272 °C dec; IR 2215 cm^{-1}; ^{1}H NMR (200 MHz, CDCl$_3$) δ 10.21 (s, 1 H), 8.82 (dd, J = 7.5, 1.2 Hz, 1 H), 8.80 (dd, J = 5.2, 1.8 Hz, 1 H), 7.98 (ddd, J = 7.5, 7.5, 1.8 Hz, 1 H), 7.82 (s, 2 H), 7.51 (ddd, J = 7.5, 5.2, 1.2 Hz, 1 H); MS (25 eV, 120 °C) m/z (relative intensity) 334 (M$^+$ + 1, 21), 333 (M$^+$, 100), 332 (M$^+$ – 1, 93), 307 (M$^+$ – CN, 14).

Anal. Calcd for C$_{19}$H$_7$N$_7$·0.75H$_2$O: C, 65.80; H, 2.47; N, 28.27. Found: C, 65.96; H, 2.38; N, 28.21.

1e: yield 14%, yellow powder (1,2-dichloroethane); mp 201–210 °C dec; IR 2212 cm^{-1}; ^{1}H NMR (200 MHz, CDCl$_3$) δ 9.62 (s, 1 H), 9.53 (br s, 1 H), 8.90 (d, J = 7.2 Hz, 1 H), 8.89 (d, J = 7.2 Hz, 1 H), 7.84 (s, 2 H), 7.66 (dd, J = 7.2, 7.2 Hz, 1 H); MS (13.5 eV, 110 °C) m/z (relative intensity) 334 (M$^+$ + 1, 20), 333 (M$^+$, 100).

Anal. Calcd for C$_{19}$H$_7$N$_7$·H$_2$O: C, 64.96; H, 2.58; N, 27.91. Found: C, 65.26; H, 2.12; N, 27.89.

1f: yield 20%, yellow powder (1,2-dichloroethane); mp 290–310 °C dec; IR 2211 cm^{-1}; ^{1}H NMR (200 MHz, CDCl$_3$) δ 9.62 (s, 1 H), 8.95 (AA'XX', $J_{2,3}$ = 5.5 Hz, 2 H), 8.27 (AA'XX', $J_{2,3}$ = 5.5 Hz, 2 H), 7.86 (s, 2 H); MS (13.5 eV, 130 °C) m/z (relative intensity) 334 (M$^+$ + 1, 21), 333 (M$^+$, 100).

Anal. Calcd for C$_{19}$H$_7$N$_7$·H$_2$O: C, 64.96; H, 2.58; N, 27.91. Found: C, 65.00; H, 2.31; N, 27.84.

1g: yield 53%, red cubes (1,2-dichloroethane); mp 280–285 °C dec; IR 2215 cm^{-1}; ^{1}H NMR (200 MHz, CDCl$_3$) δ 8.50 (d, J = 8.0 Hz, 2 H), 8.29 (dd, J = 4.8, 1.2 Hz, 2 H), 7.96 (dd, J = 8.0, 7.8 Hz, 2 H), 7.81 (br s, 2 H), 7.31 (dd, J = 7.8, 4.8 Hz, 2 H); UV (MeCN) λmax 392 nm (log ϵ 4.68), 372 (4.56), 352 (4.45), 284 (3.99), 268 (4.01), 240 (4.31); MS (13.5 eV, 130 °C) m/z (relative intensity) 410 (M$^+$, 100), 409 (M$^+$ – 1, 41).

Anal. Calcd for C$_{24}$H$_{10}$N$_6$: C, 70.24; H, 2.46; N, 27.30. Found: C, 70.30; H, 2.62; N, 27.11.

1h: yield 12%, yellow powder (1,2-dichlorobenzene); mp 345–360 °C dec; IR 2216 cm^{-1}; ^{1}H NMR could not be measured because of its very low solubility; MS (13.5 eV, 170 °C) m/z (relative intensity) 409 (M$^+$ + 1, 72), 408 (M$^+$, 100).

Anal. Calcd for C$_{24}$H$_8$N$_8$·0.5H$_2$O: C, 69.06; H, 2.17; N, 26.85. Found: C, 69.46; H, 2.14; N, 26.58.

1i: yield 32%, orange fibers (CH$_2$Cl$_2$/n-hexane); mp 280–282 °C dec; IR 2212 cm^{-1}; ^{1}H NMR (200 MHz, CDCl$_3$) δ 7.70 (s, 2 H), 3.27 (d, J = 4.4 Hz, 1 H), 2.41 (ddd, J = 9.2, 9.2, 4.2 Hz, 1 H), 2.17 (dd, J = 9.2, 9.2 Hz, 1 H), 1.30–1.50 (m, 2 H), 1.46 (s, 3 H), 1.15 (s, 3 H), 0.66 (s, 3 H); MS (70 eV) m/z (relative intensity) 364 (M$^+$, 68), 349 (100); [α]$^{20}_D$ = +24° (c 1.0, CHCl$_3$).

Anal. Calcd for C$_{22}$H$_{16}$N$_6$·H$_2$O: C, 69.10; H, 4.74; N, 21.98. Found: C, 69.29; H, 4.59; N, 22.36.

Preparation of Anion Radical Salts of Pyrazino-TCNQs (1a–c). To a hot solution of 1a (32.7 mg, 0.128 mmol) in MeCN (10 mL) was added a solution of Et$_4$NI (100.6 mg, 0.391 mmol) in 5 mL of MeCN. After cooling, black fibers of Et$_4$N$^+$(1a)$_2$$^{•-}$ (1:2) salt were filtered.

Tetraethylammonium salts of 1b$^{•-}$ and 1c$^{•-}$ were similarly obtained by the reactions of 1b and 1c with Et$_4$NI in MeCN, respectively. Reaction of 1b with NaI also gave Na$^+$(1b)$^{•-}$ with a 1:1 molar ratio.

Et$_4$N$^+$(1a)$_2$$^{•-}$: mp >400 °C; IR 2156 cm^{-1}; UV (MeCN) λmax 834 nm (log ϵ 4.23), 642 (4.67), 595 (4.21), 389 (4.83), 369 (4.79), 350 (4.58, sh), 286 (4.23, sh), 278 (4.26), 233 (4.32); UV (DMF) λmax 843 nm (log ϵ 4.38), 649 (4.81), 602 (4.36), 558 (4.11), 368 (4.47), 355 (4.43), 316 (4.09), 289 (4.34); σ_{RT} = 6.7 × 10^{-4} S cm^{-1}.

Anal. Calcd for C$_{36}$H$_{22}$N$_{13}$: C, 67.28; H, 4.39; N, 28.33. Found: C, 67.49; H, 4.46; N, 28.23.

Et$_4$N$^+$(1b)$_2$$^{•-}$: black fibers; mp 221–225 °C dec; IR 2177, 2157 cm^{-1}; σ_{RT} = 2.0 × 10^{-8} S cm^{-1}.

Anal. Calcd for C$_{40}$H$_{36}$N$_{13}$·0.5H$_2$O: C, 67.88; H, 5.27; N, 25.73. Found: C, 68.07; H, 5.09; N, 25.44.

Et$_4$N$^+$(1c)$_2$$^{•-}$: green-black solid; mp 255–256 °C dec; IR 2177 cm^{-1}; UV (MeCN) λmax 839 nm (log ϵ 4.09), 656 (4.61), 604 (4.07),

472 (3.93), 392 (4.79), 372 (4.84), 354 (4.74), 280 (4.39), 228 (4.77); σ_{RT} = 1.2 × 10^{-4} S cm^{-1}.

Anal. Calcd for C$_{80}$H$_{44}$N$_{13}$: C, 76.09; H, 4.68; N, 19.23. Found: C, 75.82; H, 4.81; N, 19.35.

Na$^+$(1b)$^{•-}$: black fibers; mp 210–215 °C dec; IR 2188, 2163 cm^{-1}; UV (MeCN) λmax 827 nm (log ϵ 4.36), 742 (3.81), 620 (4.55), 578 (4.15, sh), 361 (4.26), 348 (4.02), 288 (4.06, sh), 279 (4.08), 236 (4.01); σ_{RT} = 7.7 × 10^{-4} S cm^{-1}.

Anal. Calcd for C$_{16}$H$_8$N$_6$Na·2H$_2$O: C, 55.98; H, 3.52; N, 24.48. Found: C, 55.01; H, 3.23; N, 24.38.

Preparation of CT Crystals of Pyrazino-TCNQ (1a). To a solution of 1a (38.2 mg, 0.149 mmol) in hot CH$_2$Cl$_2$ (10 mL) was added TTF (31.1 mg, 0.147 mmol), and the mixture was heated for a few minutes. After cooling, the TTF·1a (1:1) complex was obtained as a black solid, mp >400 °C; IR 2182 cm^{-1}.

Anal. Calcd for C$_{20}$H$_8$N$_6$S$_4$: C, 52.16; H, 1.75; N, 18.25; S, 27.84. Found: C, 51.84; H, 1.98; N, 18.13; S, 27.67.

The TMTSF·1a (1:1) complex was similarly obtained as a black powder by the direct method in CH$_2$Cl$_2$: mp >400 °C; IR 2191 cm^{-1}.

Anal. Calcd for C$_{24}$H$_{16}$N$_6$Se$_4$: C, 40.93; H, 2.29; N, 11.93. Found: C, 40.24; N, 2.18; N, 11.70.

Preparation of N-Methylated Cations (2$^+$). Under a nitrogen atmosphere methyl triflate (TfOMe) (82.9 mg, 0.505 mmol) was added to a boiling solution of 1d (56.0 mg, 0.168 mmol) in dry 1,2-dichloroethane (20 mL). The mixture was heated under reflux for 27 h, giving a greenish yellow powder of 2-(2-(5H,8H-5,8-bis(dicyanomethylene)quinoxalyl))-1-methylpyridinium triflate (2d$^+$TfO$^-$) (41.6 mg) in 50% yield.

Triflate salts of 2e$^+$, 2f$^+$, and 2g$^+$ were similarly prepared by the reactions of 1e, 1f, and 1g with TfOMe, respectively. In the case of 2g$^+$, CH$_2$Cl$_2$ was used as a solvent. N-Methylation of 1h giving 10H,13H-10,13-bis(dicyanomethylene)-4-methylpyrido-[2,3-f]quinoxalo[2,3-h]quinolinium (2h$^+$) was attempted using TfOMe and Me$_2$SO$_4$.

2d$^+$TfO$^-$: mp 195–200 °C dec; IR 2217 cm^{-1}; ^{1}H NMR (200 MHz, acetone-d_6) δ 9.75 (s, 1 H), 9.49 (d, J = 6.4 Hz, 1 H), 9.03 (dd, J = 7.4, 7.4 Hz, 1 H), 8.78 (d, J = 7.4 Hz, 1 H), 8.53 (dd, J = 7.4, 6.4 Hz, 1 H), 8.07 (s, 2 H), 4.80 (s, 3 H); FAB MS (nitrobenzyl alcohol matrix) (relative intensity) 351 (M$^+$ + 3, 29), 350 (M$^+$ + 2, 100) 349 (M$^+$ + 1, 83), 348 (M$^+$, 76).

Anal. Calcd for C$_{21}$H$_{10}$N$_7$F$_3$O$_3$S·0.5H$_2$O: C, 49.81; H, 2.19, N, 19.36. Found: C, 49.80; H, 2.30; N, 19.28.

2e$^+$TfO$^-$: yield 53%, greenish yellow powder; mp 247–250 °C dec; IR 2213 cm^{-1}; ^{1}H NMR (200 MHz, acetone-d_6) δ 10.18 (s, 1 H), 10.07 (s, 1 H), 9.73 (d, J = 8.2 Hz, 1 H), 9.39 (d, J = 6.0 Hz, 1 H), 8.58 (dd, J = 8.2, 6.0 Hz, 1 H), 8.05 (s, 2 H), 4.78 (s, 3 H); FAB MS (nitrobenzyl alcohol matrix) (relative intensity) 350 (M$^+$ + 2, 25) 349 (M$^+$ + 1, 57), 348 (M$^+$, 100).

Anal. Calcd for C$_{21}$H$_{10}$N$_7$F$_3$O$_3$S·0.25H$_2$O: C, 50.25; H, 2.11; N, 19.53. Found: C, 50.31; H, 2.13; N, 19.31.

2f$^+$TfO$^-$: yield 31%, greenish yellow powder; mp 234–240 °C dec; IR 2213 cm^{-1}; ^{1}H NMR (200 MHz, acetone-d_6) δ 10.14 (s, 1 H), 9.44 (AA'BB', $J_{2,3}$ = 6.9 Hz, 1 H), 9.24 (AA'BB', $J_{2,3}$ = 6.9 Hz, 1 H), 8.04 (br s, 2 H), 4.75 (s, 3 H); FAB MS (nitrobenzyl alcohol matrix) (relative intensity) 351 (M$^+$ + 3, 16), 350 (M$^+$ + 2, 59), 349 (M$^+$ + 1, 77), 348 (M$^+$, 100).

Anal. Calcd for C$_{21}$H$_{10}$N$_7$F$_3$O$_3$S·1.5H$_2$O: C, 48.10; H, 2.50; N, 18.70. Found: C, 48.38; H, 2.20; N, 18.53.

2g$^+$TfO$^-$: yield 54%, yellow plates; mp 225–226.5 °C dec; IR 2213 cm^{-1}; ^{1}H NMR (200 MHz, acetone-d_6) δ 9.43 (ddd, J = 6.5, 1.2, 1.0 Hz, 1 H), 8.89 (ddd, J = 7.8, 1.2, 1.0 Hz, 1 H), 8.80 (ddd, J = 8.2, 6.2, 1.2 Hz, 1 H), 8.43 (dd, J = 6.5, 6.2 Hz, 1 H), 8.36 (ddd, J = 4.8, 1.8, 1.0 Hz, 1 H), 8.23 (dd, J = 8.2, 1.0 Hz, 1 H), 8.14 (ddd, J = 7.8, 7.6, 1.8 Hz, 1 H), 8.08 (br s, 2 H), 7.56 (ddd, J = 7.6, 4.8, 1.2 Hz, 1 H), 4.58 (s, 3 H); UV (MeCN) λmax 396 nm (log ϵ 4.70), 376 (4.57), 350 (4.36), 330 (4.22, sh), 274 (4.10), 242 (4.21); FAB MS (nitrobenzyl alcohol matrix) (relative intensity) 427 (M$^+$ + 2, 100), 426 (M$^+$ + 1, 76), 425 (M$^+$, 57).

Anal. Calcd for C$_{26}$H$_{13}$N$_8$F$_3$O$_3$S: C, 54.36; H, 2.28; N, 19.50. Found: C, 54.22; H, 2.31; N, 19.32.

Preparation of Neutral Radicals 3. To a solution of 2d$^+$-TfO$^-$ (32.7 mg, 0.0657 mmol) in dry MeCN (5 mL) was added a solution of n-Bu$_4$NI (120.9 mg, 0.327 mmol) in dry MeCN (5 mL), and the mixture was heated under reflux for a few minutes. After cooling, a black powder was filtered and washed with dry
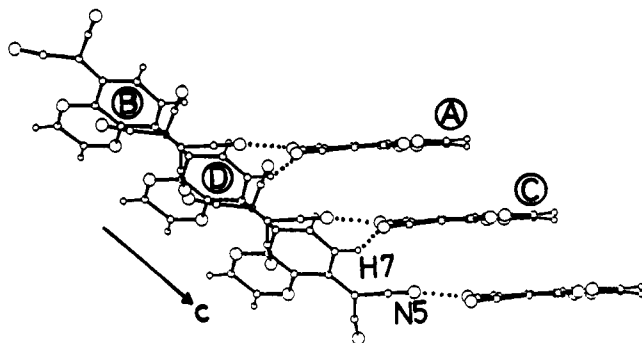
Figure 4. Catemer formation of **1a** by C—H···N≡C contacts along the *c* axis. Viewed parallel to the best plane of molecule A (or C). π-Orbitals of molecules A and C are scarcely overlapped. C(7)–H(7)···N(5)≡C(13) (2.54 Å) contacts are shown by broken line, and those of C(8)—H(8)···N(5)≡C(13) (2.84 Å) were omitted for clarity. Symmetry operations are as follows: A (*x*, *y*, *z*); B (–$^1/_2$ – *x*, 1 – *y*, –$^1/_2$ + *z*); C (*x*, 1 + *y*, *z*); D (–$^1/_2$ – *x*, 1 – *y*, $^1/_2$ + *z*).

MeCN to give 2-(2-(5*H*,8*H*-5,8-bis(dicyanomethylene)-quinoxalyl))-1-methylpyridyl (**3d**) (12.5 mg) in 55% yield.

Radicals **3e**, **3f**, and **3g** were similarly prepared by the reactions of triflate salts of **2e⁺**, **2f⁺**, and **2g⁺**, respectively, with *n*-Bu₄NI in MeCN.

3d: mp 240–245 °C dec; IR 2182 cm⁻¹; UV (DMF) λmax 849 nm (log ε 3.60), 699 (4.34), 640 (3.94), 582 (3.87), 464 (3.72), 374 (4.07), 356 (4.05), 312 (4.22); MS spectrum could not be obtained in FAB, EI, and DEI modes.
Anal. Calcd for $C_{20}H_{10}N_7$·0.25H_2O; C, 68.08; H, 3.00; N, 27.79. Found: C, 67.90; H, 3.09; N, 27.58.

3e: yield 93%, black-violet powder; mp 240–250 °C dec; IR 2174 cm⁻¹; UV (MeCN) λmax 842 nm (log ε 3.57), 696 (4.26), 580 (3.81), 458 (3.75), 378 (4.07), 316 (4.36); MS spectrum could not be obtained in FAB, EI, and DEI modes.
Anal. Calcd for $C_{20}H_{10}N_7$·0.75H_2O; C, 66.38; H, 3.20; N, 27.10. Found: C, 66.49; H, 3.13; N, 26.92.

3f: yield 66%, black-violet powder; mp 150–155 °C dec; IR 2173 cm⁻¹; MS spectrum could not be obtained in FAB, EI, and DEI modes.
Anal. Calcd for $C_{20}H_{10}N_7$·1.75H_2O; C, 63.24; H, 3.58; N, 25.81. Found: C, 63.54; H, 3.44; N, 25.18.

3g: yield 70%, deep violet plates; mp 205–206 °C dec; IR 2177 cm⁻¹; UV (MeCN) λmax 847 nm (log ε 3.76), 696 (4.53), 636 (4.07), 447 (3.75), 380 (4.26), 358 (4.19), 322 (4.33), 282 (4.25); FAB MS (nitrobenzyl alcohol matrix) (relative intensity) 426 (M⁺ + 1, 7), 425 (M⁺, 14), 410 (M⁺ + 1 – CN, 72), 409 (M⁺ – CN, 100).
Anal. Calcd for $C_{25}H_{13}N_8$·1.25H_2O; C, 67.03; H, 3.49; N, 25.02. Found: C, 66.83; H, 3.57; N, 25.13.

X-ray Structural Analysis of Pyrazino-TCNQ (1a). A yellow platelike crystal with approximate dimensions of 0.1 × 0.3 × 0.3 mm was grown by gradient sublimation (220 °C, 1 × 10⁻² Torr) onto Teflon. Crystal data were as follows: MF $C_{14}H_4N_6$, MW 256.23, orthorhombic, $P2_12_12_1$, *a* = 14.559 (1) Å, *b* = 10.442

(1) Å, *c* = 7.913 (1) Å, *V* = 1202.9 (2) Å³, *Z* = 4, D_c = 1.42 g cm⁻³, μMo Kα = 0.871 cm⁻¹. Reflection data were collected on an AFC-5R (45 kV, 200 mA) diffractometer at 13 °C by using graphite monochromated Mo Kα radiation (λ = 0.710 49 Å). A total of 1761 independent reflections were collected within 2θ < 57°. The structure was solved by the direct method (RANTAN81 program)[26] and refined by the block-diagonal least-squares method using anisotropic temperature factors for non-hydrogen atoms. All of the hydrogen atoms were found in the D map and refined isotropically. The final *R* value was 0.0435 for 1329 reflections with $|F_o| > 3\sigma |F_o|$. The estimated standard deviations for the bond distances and angles were 0.004–0.006 Å and 0.2–0.4°, respectively. All calculations were carried out on an ACOS 2020 computer at Tohoku University by using applied library programs of UNICSIII system.[27]

There exist two kinds of C–H···N≡C contacts in the crystal, and the distances of H···N and angles for H···N≡C are 2.54 Å and 134.0° for C(7)—H(7)···N(5)≡C(13) and 2.84 Å and 172.1° for C(8)—H(8)···N(5)≡C(13) contacts, respectively. Although the latter contact is longer than the sum of the van der Waals radii of H···N (2.75 Å),[28] the linearity of the H–N–C atomic array suggests the important contribution of weak C–H···N hydrogen bonds.[29] These weak bonding interactions connect the molecules around the 2-fold screw axis along the *c* axis (Figure 4), and the resulting catemers are packed in a herringbone pattern in the crystal.

Measurement of Redox Potentials. Redox potentials of 1–3 were measured by cyclic voltammetry in dry DMF containing 0.1 mol dm⁻³ Et₄NClO₄ as a supporting electrolyte. All values shown in the text and tables are in *E*/V vs SCE, and were measured under the same conditions by using Pt wire as a working electrode. In the case of irreversible waves, half-wave potentials were estimated from the cathodic peak potentials (E^{pc}) as $E^{red} = E^{pc} + 0.03$ V.

Supplementary Material Available: Listings of positional and thermal parameters, bond lengths and angles, and description and drawing of crystal structure of **1a** and listings of molar ratios, melting points, electrical conductivities, and analytical values for CT crystals of **1a–c** (6 pages). This material is contained in many libraries on microfiche, immediately follows this article in the microfilm version of the journal, and can be ordered from the ACS; see any current masthead page for ordering information.

(26) Jia-xing, Y. *Acta Crystallogr. Sect. A* **1981**, *37*, 642; **1983**, *39*, 35.
(27) Sakurai, T.; Kobayashi, K. *Rikagaku Kenkyusho Hokoku* **1979**, *55*, 69.
(28) Bondi, A. *J. Phys. Chem.* **1964**, *68*, 441.
(29) Taylor, R.; Kennard, O. *J. Am. Chem. Soc.* **1982**, *104*, 5063.